

Energy relaxation in a vacuum capacitor: sequential time constants and unequal currents entering and leaving the capacitor

Frank V. Kowalski*

Physics Department, Colorado School of Mines, Golden CO. 80401 U.S.A.

(Dated: January 20, 2023)

Abstract

A resistor-capacitor circuit is shown to decay non-exponentially and to have unequal currents flowing into and out of the capacitor. Relaxation of the stored energy can involve multiple sequential relaxation processes (with dramatically different time constants), separated by a transition region that involves a change in current direction. This is demonstrated using a vacuum capacitor to eliminate the effect of a dielectric between the plates (although a ceramic capacitor shows a similar effect). A possible mechanism for such a response is illustrated in a related decay of polypropylene capacitors.

* fkowalsk@mines.edu

I. INTRODUCTION

Energy redistribution is intrinsic to all dynamical systems. The energy of interest here is that stored in a capacitor. Capacitors are essential lumped-element or inherent components of every electronic system or device. Their fidelity as sensors impacts the viability of scientific models. The electro-mechanical coupling that causes motion of the plates in a capacitor is used to probe foundational issues in quantum mechanics.[1, 2] In addition, some quantum computers utilize capacitors as fundamental components.[3, 4] Energy relaxation is crucial to the function of these devices. Therefore, one might expect that a thorough understanding of a capacitor exists. Data are presented below to illustrate that this remains an open problem.

The capacitor's response is modeled with Kirchhoff's current and voltage laws. When applied in quasi-steady state these predict the ideal behavior associated with equal and opposite charges on the capacitor plates and exponential decay in an RC circuit. The same current then flows into one terminal of the capacitor and out of the other.

However, non-ideal behavior is found in a practical device. For example, non-exponential decay was first studied during the 1850's using Leyden jars and modeled with stretched exponential functions.[5] This response is attributed to the dielectric. The literature is replete with studies illustrating such non-ideal behavior.[6, 7] Circuit simulation software typically accounts for this non-ideal behavior of the capacitor by using a lumped circuit model that is comprised of ideal inductors, resistors, and capacitors.

An example of one relaxation mechanism involves energy stored in the polarization of the dielectric contained within a capacitor that is released as the alignment of the dipoles dissipates. Consider the time domain method of measuring such an effect where a voltage, having energized an RC circuit, is removed. The charge induced on the capacitor plates by this polarization then becomes a source of currents that flow through an external resistor as the polarization decays. The difficulty in modeling this process increases when the relaxation mechanism is affected by the rate of change of the electric field in the dielectric.[8] Nevertheless, the decay in this circuit is used to probe the microscopic structure of the dielectric, a method widely applied in material science and chemistry.[6, 9, 10].

Another common mechanism associated with non-ideal behavior is electro-mechanical coupling.[11] Yet another non-ideal effect involves the electronic properties of the conducting plates leading to a quantum treatment of capacitance. [12].

The purpose here is to document the non-ideal behavior of a capacitor whose relaxation is unaffected by a dielectric. Although a model that the data supports is not given, evidence of a potential mechanism responsible for the observed relaxation, related to the attraction between positive and negative charges on the capacitor plates [13, 14], is presented.

II. RESULTS

Fig. 1 illustrates the decay currents through $R_1 = 3930 \Omega$ (solid) and $R_2 = 3920 \Omega$ (dashed), respectively, for the circuit shown in the inset. The vacuum capacitor has $C = 505 \text{ pF}$ while $V = 9.4$. M_1 and M_2 represent the meters that measure the voltages (and therefore the currents from Ohm's law) through R_1 and R_2 .

The mathematical form of the RC decay as a function of time is expected to be exponential and therefore the data is most often presented in a semi-log plot. However, since the current changes direction, this is modified using the logarithm of the absolute value of the current. The interpretation of such graphs is best illustrated using the currents shown in fig. 1(a) and fig. 1(b). The dips in the semi-log plots correspond to the zero currents in fig. 1(a). After going negative (reversing direction) the current then slowly approaches zero which is indicated in the semi-log plot by a downward slope.

In addition to illustrating the vacuum capacitor decay data, the solid circles in frame (b) show the decay data from a 509 pF ceramic capacitor for the same values of R_1 and R_2 . Although the currents through R_1 and R_2 for the ceramic capacitor are both represented by solid circles in this figure, they are easily separated by the context in which they appear. The unequal current flow into and out of a capacitor therefore appears to be a universal characteristic of capacitors.

The dot-two-dash line in fig. 1(b) represents the expected exponential decay. However, since it overlaps with the decay data for the first few time constants it has been offset along the ordinate to better distinguish it. Frame fig. 1(c) illustrates data from the same circuit over 200 time constants. The lower curve only shows data for $\log_e |I_{R_2}|$ from 0 to 80 time constants to prevent overlap between it and the data from $\log_e |I_{R_1}|$. The repeatability of this raw data is illustrated by its fluctuations. The baseline of the A/D converter corresponds to $\log_e |I_R| \approx -16$.

Fig. 2 presents decay data for the circuit shown in fig. 1(a) with the same vacuum

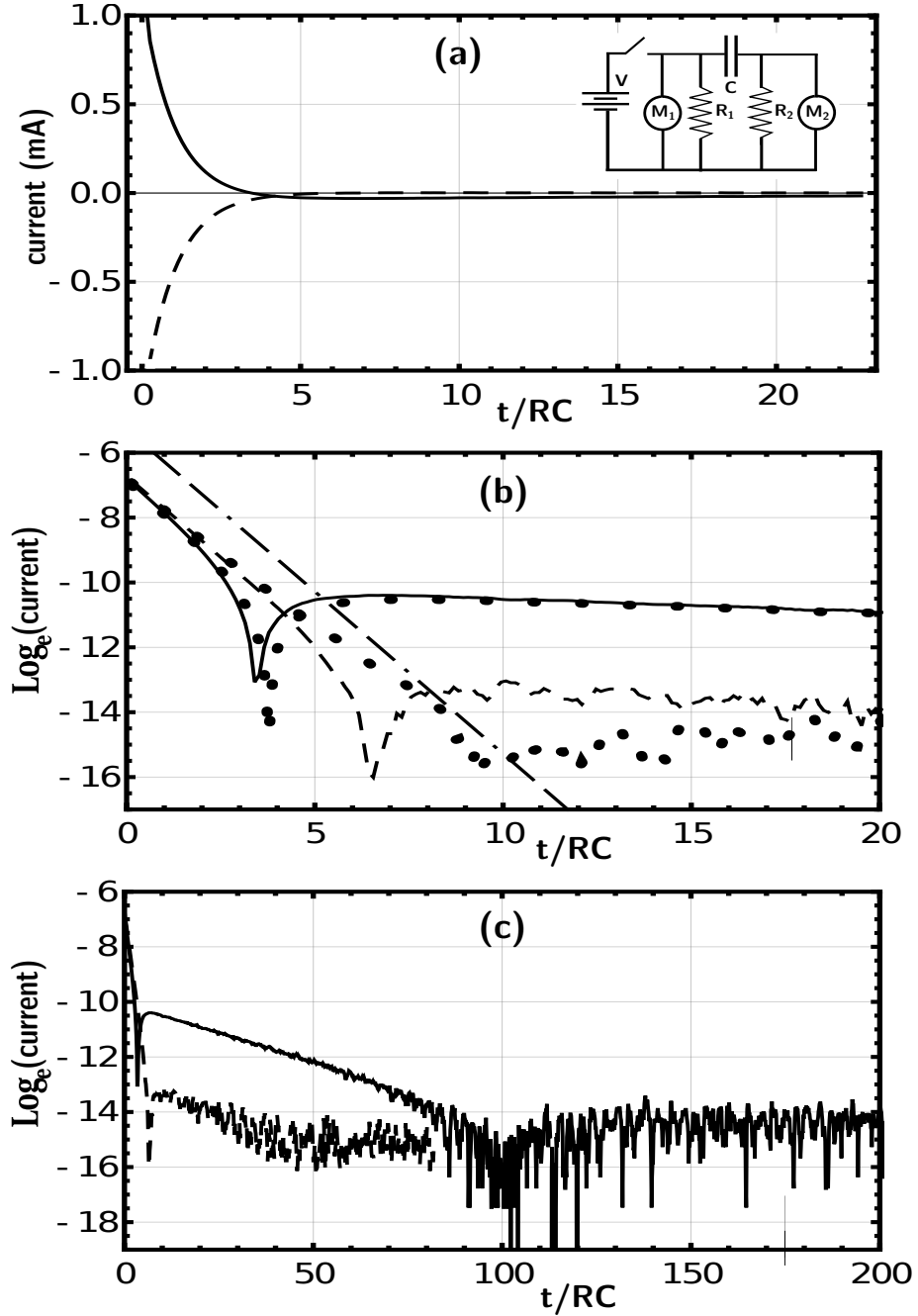


FIG. 1. Current relaxation data through the two resistors of the circuit shown in the inset using 505 pF vacuum capacitor with $R_1 = R_2$. A linear scale is used in (a) while $\log_e |I_{R_1}|$ (solid) and $\log_e |I_{R_2}|$ (dashed) lines illustrate the decay in figs. (b) and (c). The solid circles in (b) show data for a 509 pF ceramic capacitor. All traces are raw data for a single decay.

capacitor and $R_2 = 0$ while $R_1 = 861, 7850, 27000, 63000$, and 91600Ω . These are presented with the smallest to largest resistor values from top to bottom at $t/RC = 0$ in fig. 2(a). The same order is shown in fig. 2(b) without the $R_1 = 91600 \Omega$ data. Each trace is an average over four decays. A moving average over 20 data points (2000 data points per trace) in frame (b) has been applied to the tails of the data to mitigate overlap of the traces.

Prominent characteristics of this data are (I) three relaxation times (before and after each dip as shown in fig. 2(a) and (II) two zero current dips for each trace as shown in fig. 2(b) (the second dip for the upper trace is not shown since it occurs at $t/RC = 930$).

Apart from the transition or zero crossing region the data support exponential decay involving an initial relaxation time $\tau_1 = RC$ and later relaxation times that are functions of RC . The second relaxation time is $\tau_2 = F_2(RC)\tau_1$. Fig. 2 (c) shows the relationship between τ_1 and τ_2 in a plot of $1/F_2(RC \times 10^6)$, as a function of $RC \times 10^6$. The data support within error a linear correlation, $1/F_2(RC \times 10^6) = [0.000 \pm 0.006] + [0.0026 \pm 0.0011]RC \times 10^6$.

The times at which the two dips (zero current crossings) occur for each trace are given by T_1 and T_2 . Fig. 2(d) plots $1/T_1$ (the lower line with a positive slope) and $1/T_2$ (the upper line with negative slope) as a function of $RC \times 10^6$. The scale on the left hand ordinate corresponds to the $1/T_1$ data while that on the right hand ordinate corresponds to the $1/T_2$ data. These data support within error the linear relationships, $1/T_1 = [0.000068 \pm 0.006] + [0.0026 \pm 0.001]RC \times 10^6$ and $1/T_2 = [0.247 \pm 0.008] + [-0.003 \pm 0.0004]RC \times 10^6$.

The third sequential exponential relaxation occurs as shown in fig. 2(b). Data for $R_1 = 7850, 27000, 63000 \Omega$ are used to calculate the linear correlation, $1/F_3(RC \times 10^6) = [0.0007 \pm 0.0008] + [0.0003 \pm 0.00006]RC \times 10^6$.

To further illustrate the behavior of the capacitor with $R_1 = R_2$ (values equal within 1%), a variable air capacitor, set at 240 pF, was charged to 19.8 V. The current oscillations for different resistance pair values over 40 time constants are shown in fig. 3 (a) and 18 time constants in (b), (c), and (d). Up to four raw data results for each pair of resistors are superimposed to illustrate repeatability of the data.

While the small differences in these currents through R_1 and R_2 on a time scale greater than two time constants are given in fig. 3, larger differences for shorter time scales are shown in fig. 4. The data are presented as a percent change in the currents flowing into and out of the capacitor, $\Delta\text{Current}(\%) = (I_{R_1} - I_{R_2})/I_0$ where I_0 is the current through R_1 long after the circuit has been energized but before the decay. Again multiple traces for each

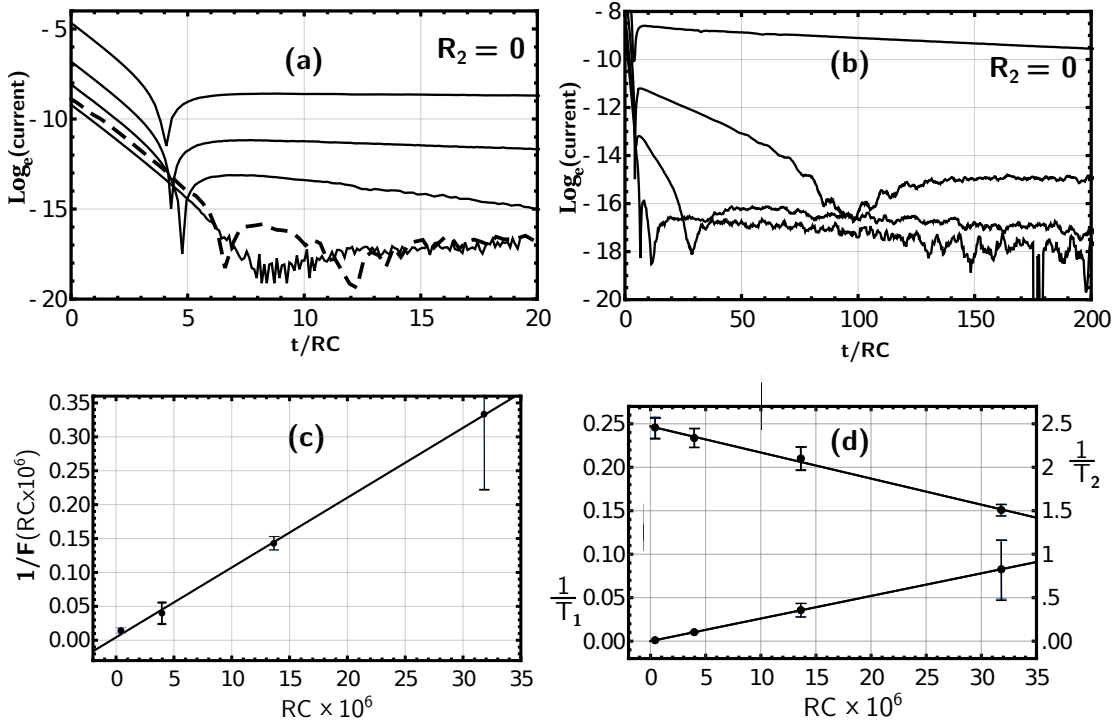


FIG. 2. Decay data for the circuit in fig. 1 with $R_2 = 0$ and increasing values of R_1 from top to bottom in (a) and (b). Frame (c) illustrates an inverse relationship between the second relaxation time as a function of the first relaxation time from the data in (a) and (b). Frame (d) shows an inverse relationship between the time at which the first (lower line) and the second (upper line) dips occur as a function of the relaxation time.

value of the resistance are presented.

The charge on each plate can be calculated by integrating the currents flowing into and out of the resistor connected to that plate. The net charge on the plates, $Q[t]$, varies as $dQ[t]/dt = I_{R_1} - I_{R_2}$, the functional form of which is shown in fig. 4.

Fig. 5 illustrates these decays over the full variation of currents using logarithmic plots.

III. ANALYSIS

The model perhaps most appropriate for exponential decay is that of the self capacitance associated with a charged sphere. The rate at which its charge decays through a resistor to infinity is proportional to charge on the sphere. However, the mutual capacitance associated

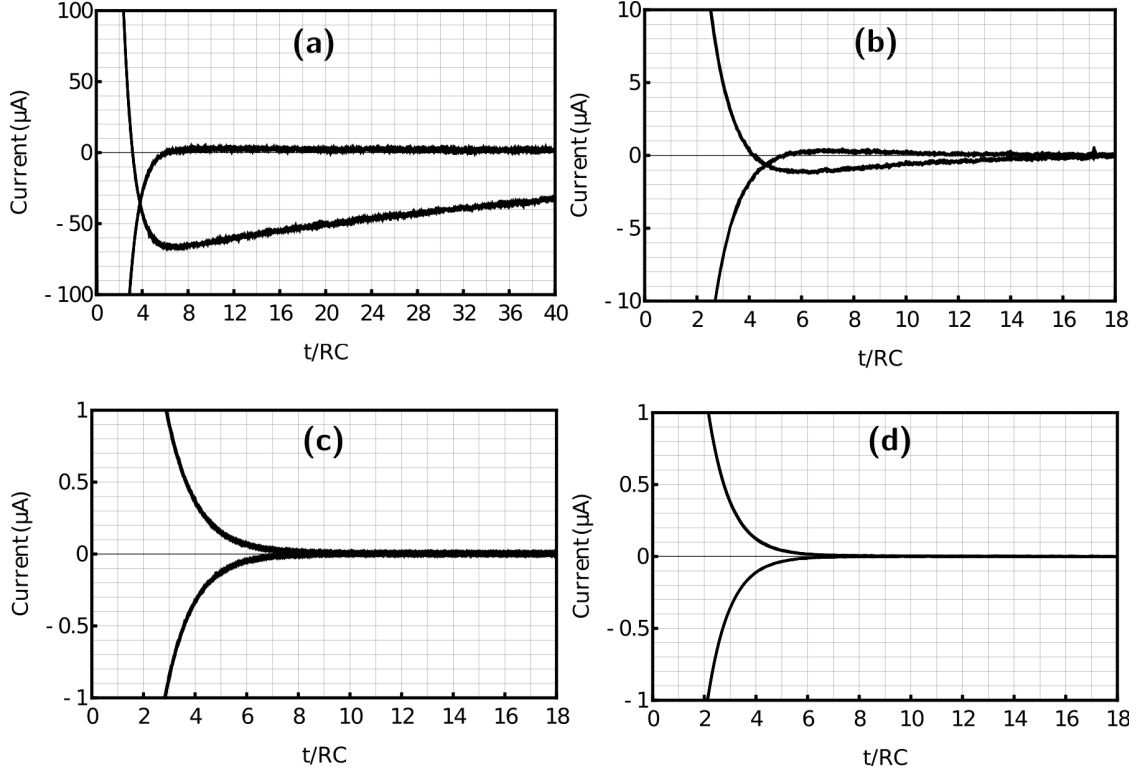


FIG. 3. Data for the 240 pF air capacitor used in the circuit shown in fig. 1. Currents through R_1 (the upper trace at $t/RC = 1$) and $R_2 = R_1$ for resistor pair values of 4.7 K Ω , 47 K Ω , 225 K Ω , and 704 K Ω are shown in frames (a), (b), (c), and (d), respectively.

with two such neighboring spheres adds an interaction term.

Such an interaction is also associated with the attraction between induced positive and negative charges on the capacitor plates. Fig. 6 illustrates this effect using the circuit shown in the inset of frame (d).

This circuit isolates the right plate of C_1 from ground potential using capacitor $C_2 = C_1 = C$. After the switch has been closed for multiple time constants, charge is induced on the plates of C_1 and C_2 . The switch is then opened and the voltage on the left hand plate of C_1 decays to ground potential as shown in fig. 6. However, induced charge remains on the right hand plates as indicated by the non-zero voltage with respect to ground on the $\log_e |V_{R_2}|$ trace (shown in all frames) long after the switch has been opened. If, on the other hand, this negative induced charge on the right plate of C_1 flowed to the positive induced charge on the right plate of C_2 , then V_{R_2} would be at ground potential. Although not observed in this dynamic system, such a ground potential on the right hand plates is

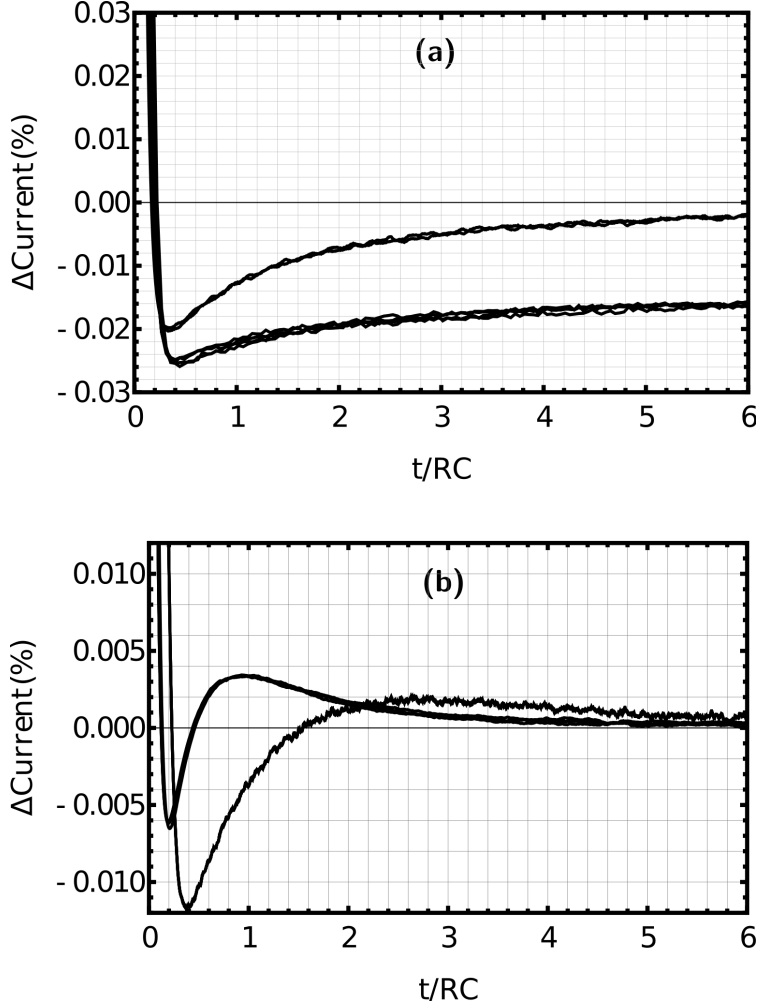


FIG. 4. The percent difference in the currents flowing into and out of the air capacitor for resistor pair values of $4.7\text{ k}\Omega$ (the lower trace in (a)), $47\text{ k}\Omega$ (upper trace in (a)), $225\text{ k}\Omega$ (the trace with the most negative minimum in (b)), and $704\text{ k}\Omega$ (the remaining trace in (b)). All traces approach zero over longer time scales.

predicted in the context of electrostatics. [15, 16].

To quantify this persistent voltage (long after the switch is opened), for $R_1 = 1801\ \Omega$, $R_2 = 158\ \Omega$, and battery voltages $V_0 = 5, 20, 40\ \text{V}$, the ratio of this offset voltage to the battery voltage was measured to be -0.0037 ± 0.0005 , -0.0034 ± 0.0003 , and -0.0036 ± 0.0002 , respectively. This ratio for the air capacitor with $C_1 = C_2 = 120\ \text{pF}$ and the same resistance values for R_1 and R_2 was measured to be -0.0023 ± 0.0002 for $V_0 = 12$. For such a measurement on the air capacitors the $10\ \text{G}\Omega$ input impedance of the voltmeter was needed to prevent the charge on the right hand plates of C_1 and C_2 from decaying through

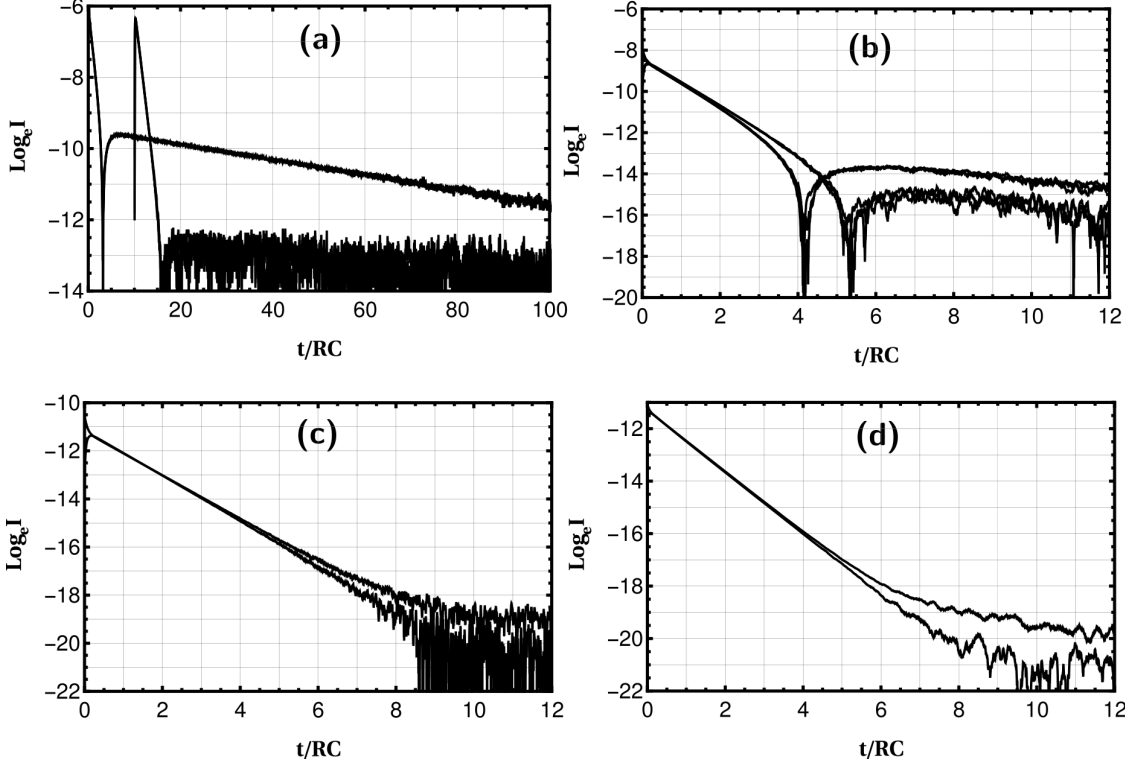


FIG. 5. Semi-log plots of the data in figs. 3. Resistor pair values of $4.7\text{K}\Omega$, $47\text{K}\Omega$, $225\text{K}\Omega$, and $704\text{K}\Omega$ are shown in frames (a), (b), (c), and (d), respectively. I_{R_1} is the higher trace at $t/RC = 100$ in frame (a) and it is the higher trace at $t/RC = 12$ in frames (b), (c), and (d). For clarity the $\log_e |I_{R_2}|$ trace in frame (a) is delayed by ten time constants.

the meter before a measurement could be made.

A linear relationship therefore exists between the energizing battery voltage and the voltage that persists on the capacitors due to the attraction between the charges induced on neighboring plates. Note that this persistent voltage depends on the values of R_1 and R_2 as shown in the different frames of fig. 6.

IV. DISCUSSION

Relaxation in a first order rate process can be described by the relation $dU/dt = -U/\tau$ where U is the energy and τ is the relaxation time. In an RC circuit a simple application of Kirchhoff's law associates U with the energy stored in the capacitor and $\tau = RC$. Integrating the power dissipated in the external resistor over time determines the capacitor's free energy.

For an ideal capacitor this stored energy can be deposited into the resistor on any time

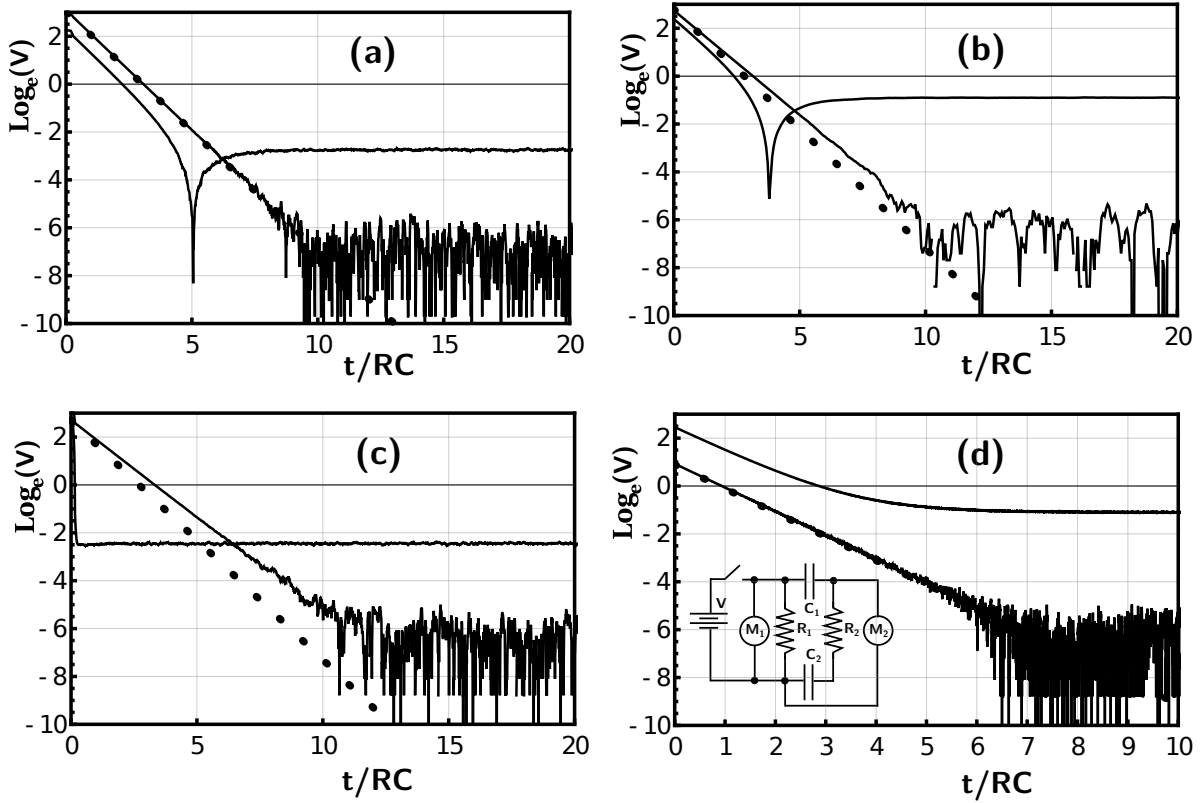


FIG. 6. Relaxation voltage data for the circuit in the inset of frame (d). Semi-log plots of $\log_e |V_{R_1}|$ (the lower trace at $t/RC = 10$) and $\log_e |V_{R_2}|$ are shown for resistor values of $R_1 = 1.801\text{K}\Omega$ and various R_2 values with capacitor values $C_1 = 2.012\mu\text{F}$ and $C_2 = 2.010\mu\text{F}$ while $V = 27$. Frames (a), (b), (c), and (d) show data for $R_2 = 158$, 1000 , 2210 , and $22219\ \Omega$, respectively. The solid circles correspond to ideal decay for the capacitors in series with a resistance $R_1 + R_2$.

scale. At one extreme is its instantaneous transfer as $R \rightarrow 0$ (this is prevented in a practical device by inductance effects). A dielectric introduces the complication of energy stored in the alignment of its dipoles. This is released into the circuit over a time scale associated with the mechanism that relaxes this dipole alignment. Individual pairs of opposite charges on the vacuum capacitor plates can also be thought of as dipoles that relax in a manner different from decay of the charges on a single spherical conductor connected to infinity via a resistor (where no dipole interaction exists).

The energy stored in the vacuum capacitor is shown in fig.1 and 2 to exponentially decay with different sequential time constants. The first matches that expected in RC decay.

The second, proportional to $F_2(RC)$, is plotted in fig. 2(c) as $1/F_2(RC) = \beta RC$, where β is a constant. Therefore the second relaxation time is inversely proportional to the first relaxation time over the range of measured RC values. The first relaxation time decreases while the second relaxation time increases as the value of the external resistance decreases. After the second relaxation process there is a third as shown in fig. 2(b), whose time constants are also inversely proportional to those of the first. However, they are substantially larger than those of the second relaxation process, which are much larger than those of the first.

The assumption that the initial charge on the plates is equal and opposite yields a symmetric initial condition in the circuit shown in fig. 1 for $R_1 = R_2$. Yet, the resulting currents are asymmetric.

Such asymmetric results might be related to a counter-electromotive force in the circuit loops (associated with self inductance) that is generated when the switch is opened. A vacuum capacitor has both a small equivalent series resistance ($\approx 10^{-5}\Omega$) and small equivalent series inductance ($\approx 10^{-8}\text{H}$).[17] The wire loop inductance for 10^{-3}m diameter wire forming a 10^{-1}m diameter loop is $6.7 \times 10^{-7}\text{H}$. The combination of parasitic inductance from the capacitor and circuit loop inductance results in an RLC circuit resonance of order 10^7 Hz, much higher than any oscillations observed. Such inductance in series with the vacuum capacitor results in an overdamped response for $R > 75\Omega$. However, the current is observed to change direction for resistance values three orders of magnitude larger. The areas of the circuit loops were also varied by two orders of magnitude with no discernible impact on the results.

The second or right dip in fig. 2(b) moves in the same direction as does the dip in fig. 6(a) and (b) when R is increased, even though their initial time constants differ by four orders of magnitude. This similarity in response for such large variation in dI/dt is additional evidence that inductance does not play a major role in the decay process.

In addition, the resistor tolerance is one percent resulting in a potential asymmetry in the fig. 1 circuit. However, the unequal currents into and out of the capacitor illustrated above did not change noticeably in attempts to balance the resistor values by the addition of a small equalizing resistor to one side of the circuit.

An ideal RC circuit exhibits relaxation with zero final charge on each plate. The results for relaxation in the circuit of fig. 6 (capacitors and resistors in series that are typically

reduced to a single equivalent capacitor and resistor for calculational purposes) demonstrate that the charge on these plates does not go to zero. The charge that remains on the plates in fig. 6 suggests that an interaction term is missing from the standard equations describing the circuit dynamics. However, lack of such an interaction is possible in a spherical capacitor, the use of which should result in near ideal behavior.

V. CONCLUSION

The relaxation of free energy differs for each plate of a capacitor in an RC circuit. It can involve sequential exponential decays that have dramatically different relaxation times and dependences on R . Although this is demonstrated using a vacuum capacitor a ceramic capacitor shows similar effects. However, as the value of RC increases the data better match the predictions of a single exponential decay, as demonstrated in fig. 5.

The pattern of an initial decay that approximates the expected behavior of an RC circuit followed by inversions in the current flow that relax with different time constants is largely independent of the initial voltage. It appears then that the subsequent relaxations are associated with the dynamical effects due to the first relaxation: the later decays cannot be initiated without the first.

The simplicity of the exponential decay model and its ability to match the initial decay data are factors that have allowed the results presented above to have been overlooked. An additional reason involves the ubiquitous use of dielectric capacitors. The behavior described above might then be attributed to the complicated relaxation mechanisms in the dielectric rather than to fundamental characteristics of a capacitor.

Energy relaxation in dynamical systems is typically modeled as a monotonically decreasing function of time. Examples are a stretched exponential or a sum of exponential decays with different relaxation times. Here a unique relaxation is documented that involves a sequence of exponential decays with increasing time constants, each separated by a transition region that involves a change in current direction.

VI. METHODS

A mechanical switch coupled and decoupled the battery from the circuit. The two channels of oscilloscopes (Picoscope models 4262 and 4226) with either 16 bit resolution at 10 MS/s or 12 bit resolution at 50 MS/s were used to collect data. The oscilloscope probes were set on a x10 scale with an input resistance $10\text{ M}\Omega$ and a capacitance of 15 pF. A Keysight 34465A digital voltmeter with input impedance $10\text{ G}\Omega$ was also used. All the circuits used 1% metal film resistors.

A Comet vacuum capacitor model CFMN-500AAC/12-DE-G was used with the resulting data shown in figs. 1, 2, and 3. A variable air capacitor, Hammarlund model 2716-15, was used in remaining figures. Film metalized polypropylene axial capacitors were used in fig. 6.

The disk ceramic capacitor (diameter $3 \times 10^{-3}\text{ m}^2$ and thickness $2 \times 10^{-3}\text{ m}$) allowed the area enclosed by the circuit to vary from 3×10^{-4} to $3 \times 10^{-2}\text{ m}^2$. However, the data shown in fig. 1 (b) did not then change noticeably.

- [1] N. Didier and R. Fazio, “Putting mechanics into circuit quantum electrodynamics,” *Comptes Rendus Physique* **13**, 470–479 (2012).
- [2] J Teufel, Dale Li, M Allman, K Cicak, Adam Sirois, J Whittaker, and R Simmonds, “Circuit cavity electromechanics in the strong-coupling regime,” *Nature* **471**, 204–8 (2011).
- [3] A. Córcoles, J. Rozen, M. Rothwell, G. Keefe, D. Vincenzo, M. Ketchen, J. Chow, C. Rigetti, J. Rohrs, M. Borstelmann, and M. Steffen, “Energy relaxation mechanisms in capacitively shunted flux qubits,” *Bulletin of the American Physical Society* (2011).
- [4] S. Gustavsson, F. Yan, G. Catelani, J. Bylander, A. Kamal, J. Birenbaum, D. Hover, D. Rosenberg, G. Samach, A. Sears, S. Weber, J. Yoder, J. Clarke, A. Kerman, F. Yoshihara, Y. Nakamura, T. Orlando, and W. Oliver, “Suppressing relaxation in superconducting qubits by quasiparticle pumping,” *Science* **354** (2016), 10.1126/science.aah5844.
- [5] R. Kohlrausch, “Theorie des elektrischen rückstandes in der leidener flasche,” *Ann. Phys.* **167**, 56–58 (2009).
- [6] A. K. Jonscher, “Dielectric relaxation in solids,” *Journal of Physics D: Applied Physics* **32**,

R57–R70 (1999).

- [7] S. Westerlund and L. Ekstam, “Capacitor theory,” IEEE Transactions on Dielectrics and Electrical Insulation **1**, 826–839 (1994).
- [8] J. L. Swantek, T. D’Esposito, J. Brannum, and F. V. Kowalski, “Dielectric relaxation affected by a monotonically decreasing driving force: An energy perspective,” Journal of Applied Physics **130**, 154101 (2021).
- [9] F. Kramer, *Broadband Dielectric Spectroscopy* (Springer Berlin Heidelberg, 2012) pp. 48–51.
- [10] Y. Feldman, A. Puzenko, and Y. Ryabov, “Dielectric relaxation phenomena in complex materials,” Advances in Chemical Physics **133**, 1 – 125 (2005).
- [11] Y. Shkel and N. Ferrier, “Electrostriction enhancement of solid-state capacitance sensing,” Mechatronics, IEEE/ASME Transactions on **8**, 318 – 325 (2003).
- [12] T. Kopp and J. Mannhart, “Calculation of the capacitances of conductors: Perspectives for the optimization of electronic devices,” Journal of Applied Physics **106**, 064504 (2009).
- [13] B. Skinner and B. I. Shklovskii, “Anomalously large capacitance of a plane capacitor with a two-dimensional electron gas,” Phys. Rev. B **82**, 155111 (2010).
- [14] C. Berthod, H Zhang, A. F. Morpurgo, and T. Giamarchi, “Theory of cross quantum capacitance,” Phys. Rev. Research **3**, 043036 (2021).
- [15] E. M. Purcell, (*Electricity and Magnetism Vol. 2*). (McGraw Hill College, 1985) p. problem 3.8.
- [16] D. J. Griffiths, (*Introduction to Electrodynamics*). (Prentice-Hall, 1989) pp. 120–121.
- [17] Jennings Technology, “Capacitors: high voltage vacuum and gas filled,” (2009).